# XAS and XPS Characterization of Mercury Binding on Brominated Activated Carbon

**ARTICLE** *in* ENVIRONMENTAL SCIENCE AND TECHNOLOGY · MARCH 2007

Impact Factor: 5.33 · DOI: 10.1021/es062121q · Source: PubMed



**3 AUTHORS**, INCLUDING:

Kirk G Scheckel
United States Environmental Protection Age…

**147** PUBLICATIONS **3,879** CITATIONS

SEE PROFILE

*Environ. Sci. Technol.* **2007**, *41,* 1747−1752

# XAS and XPS Characterization of Mercury Binding on Brominated Activated Carbon

NICK D. HUTSON,*,† BRIAN C. ATTWOOD,†,§ AND KIRK G. SCHECKEL‡

*National Risk Management Research Laboratory, Office of Research & Development, U.S. Environmental Protection Agency, Air Pollution Prevention & Control Division, 109 T. W. Alexander Drive, Research Triangle Park, North Carolina 27711, and Land Remediation & Pollution Control Division, 26 West Martin Luther King Drive, Cincinnati, Ohio 45268*

Brominated powdered activated carbon sorbents have been shown to be quite effective for mercury capture when injected into the flue gas duct at coal-fired power plants and are especially useful when burning Western low-chlorine subbituminous coals. X-ray absorption spectroscopy (XAS) and X-ray photoelectron spectroscopy (XPS) have been used to determine information about the speciation and binding of mercury on two commercially available brominated activated carbons. The results are compared with similar analysis of a conventional (non-halogenated) and chlorinated activated carbon. Both the XAS and XPS results indicate that the mercury, though introduced as elemental vapor, is consistently bound on the carbon in the oxidized form. The conventional and chlorinated activated carbons appeared to contain mercury bound to chlorinated sites and possibly to sulfate species that have been incorporated onto the carbon from adsorbed $SO_2$. The mercury-containing brominated sorbents appear to contain mercury bound primarily at bromination sites. The mechanism of capture for the sorbents likely consists of surface-enhanced oxidation of the elemental mercury vapor via interaction with surface-bound halide species with subsequent binding by surface halide or sulfate species.

## Introduction

Mercury is a toxic, persistent pollutant that accumulates in the food chain, primarily in fish. It has been demonstrated that high levels of methylmercury in the bloodstream of unborn babies and young children may harm the developing cognitive nervous system, making the child less able to think and learn (*1*). The U.S. coal-fired power plants, with capacity of just over 300 GW, are known to be a major source of domestic anthropogenic mercury emissions. To address this, the U.S. Environmental Protection Agency (EPA), on March 15, 2005, issued the first-ever federal rule to permanently reduce mercury emissions from these plants (*2*). The Clean Air Mercury Rule (CAMR) will build on EPA's Clean Air Interstate Rule (CAIR) to significantly reduce Hg emissions. The CAMR establishes standards of performance limiting mercury emissions from new and existing coal-fired power plants and creates a market-based program that will reduce nationwide utility emissions in two distinct phases. The Phase I emission limit (from 50 tons down to 38 tons by 2010) is expected to be met as a co-benefit of controls that have been installed to remove particulate matter (PM), sulfur dioxide ($SO_2$), and nitrogen oxides ($NO_X$). This would include capture of particulate-bound mercury in PM control equipment and capture of soluble mercury compounds (e.g., $HgCl_2$) in wet flue gas desulfurization (FGD) systems. The Phase II emission limit (to 15 tons by 2018) will likely require the addition of mercury-specific control technology (*1*). The most widely tested mercury-specific control technology is the injection of a powdered activated carbon (PAC) sorbent for in-duct capture of the gas-phase mercury (*2*).

During coal combustion, mercury is released into the exhaust gas as elemental vapor, $Hg^0$ (*3*). This vapor may then continue through the flue gas cleaning equipment and exit the stack as gaseous $Hg^0$ or it may be oxidized to a compound such as $HgCl_2$, HgO etc., collectively known as $Hg^{2+}$, via homogeneous (gas−gas) or heterogeneous (gas−solid) reactions. The primary homogeneous oxidation mechanism is the reaction with gas-phase chlorine (likely a Cl radical or possibly HCl) to form $HgCl_2$. While this mechanism is thermodynamically favorable, it is thought to be kinetically limited due to rapid cooling of the flue gas stream (*3*). Heterogeneous oxidation reactions occur on the surface of fly ash and unburned carbon. It is thought that in-duct chlorination of the surface of the fly ash or unburned carbon is the first step to heterogeneous oxidation and surface binding of vapor-phase elemental mercury in the flue gas stream. This is likely the same oxidation/capture mechanism for the injected activated carbon sorbents.

While conventional powdered activated carbons have been shown to be quite effective for mercury capture when applied at plants burning chlorine-containing bituminous coals, many low-chlorine subbituminous and lignite coals produce inadequate free chlorine in the flue gas and conventional activated carbon sorbents have shown limited effectiveness when used with these coals. Prehalogenated PAC sorbents have been developed specifically for application with low-chlorine coals. At several recent full-scale demonstration tests sponsored by the U.S. Department of Energy (DOE), plants burning subbituminous coal and injecting brominated activated carbon sorbents were able to remove more than 90% of the mercury with injection rates of less than 5 lbs of sorbent per million cubic feet of flue gas. These results are in contrast to prior tests, using conventional PAC, which removed a maximum of 65% of the mercury with injection rates of 10−20 lbs of sorbent per million cubic feet of flue gas (*2*). Recent leaching tests over a broad pH range have shown that the captured mercury is very strongly bound to the activated carbon sorbents (both conventional and prehalogenated) (*4*).

The specific Hg-sorbent binding mechanisms are very complex. The gas-phase speciation of mercury, the presence of other potentially competing flue gas components, the temperature of the flue gas, and the presence and type of active binding sites on the sorbent all play a role in determining the rate and mechanism of mercury binding. In order to understand the mercury capture mechanism(s), it is important to understand the chemical and physical nature of the mercury-sorbent interaction. X-ray absorption spectroscopy (XAS), and X-ray photoelectron spectroscopy (XPS)

* Corresponding author phone: (919) 541-2968; fax: (919) 541-0554; e-mail: hutson.nick@epa.gov.
† Air Pollution Prevention & Control Division (NC).
‡ Land Remediation and Pollution Prevention Division (OH).
§ Oak Ridge Institute for Science and Education (ORISE) post-doctoral program..

10.1021/es062121q CCC: $37.00 
Published on Web 02/03/2007

are techniques that have been previously used to determine information about the speciation and binding of mercury on a variety of materials (*5*−*10*). XAS spectra can be defined by two regions which include X-ray absorption near-edge spectroscopy (XANES) and extended X-ray absorption fine structure (EXAFS) spectroscopy. XANES spectra provide information on the oxidation state and characteristics of the first neighbor coordination environment. EXAFS spectroscopy provides more robust information on the identity of nearest-neighboring elements, coordination values, and interatomic bond distances.

Huggins et al. have used XAS in order to study mercury sorption on activated carbon, including carbons impregnated with iodine and sulfur (*11,12*). Their studies revealed evidence of sorption mechanisms involving the activating compounds (S- and I-) as well as acidic species of sulfur and chlorine in the flue gas. The studies only revealed evidence of mercury binding in the oxidized state. While these studies involved an evaluation of pre-iodated and in-duct chlorinated activated carbon, there was no evaluation of the brominated activated carbons that have, to date, shown the most promise for in-flight mercury capture.

Researchers at the University of North Dakota have previously used X-ray photoemission spectroscopy (XPS) to characterize the surface of activated carbon mercury sorbents and to examine the effect of flue gas components ($SO_2$, $NO_2$, HCl, and $H_2O$) on the carbon's ability to sorb mercury (*13, 14*). However, no Hg spectra were collected due to the low surface concentration and spectral interference with silicon.

## Experimental Section

**Sorbent Preparation.** Four powdered activated carbons (PACs) were exposed to mercury in a simulated flue gas. Three of the sorbents were commercially available materials: (*1*) DARCO Hg, (*2*) DARCO Hg-LH (both from NORIT Americas, Inc., Marshall, TX), and (*3*) B-PAC (Sorbent Technologies Corp., Twinsburg, OH). The DARCO Hg is an activated carbon which is marketed specifically for removing mercury from the flue gas resulting from the combustion of high chlorine content coals. The DARCO Hg-LH is brominated and is intended for use with low chlorine content coals. The B-PAC sorbent is also brominated and is marketed for use with any coal type. The bromination (both the methods and the extent) of both the B-PAC and DARCO Hg-LH are proprietary. Thus, it is not known if the activated carbons contain surface bromine as $Br_2$, HBr, or other. The fourth sorbent, a chlorinated activated carbon (referred to here as Cl-PAC), is not commercially available. The sorbent was developed at the EPA/RTP laboratories and has shown good capacity of mercury capture. The synthesis technique, involving treatment with HCl, and the sorbent performance have been described elsewhere (*15*).

The sorbents were exposed to a simulated flue gas in a fixed-bed reactor system. Mass flow controllers and valves were used to control the flow of the component gases to provide a simulated flue gas comprised of approximately 70 vol % $N_2$, 15 vol % $CO_2$, 8% $O_2$, 7% $H_2O$ vapor, 650 ppmv $SO_2$, 280 ppmv NO, 100 ppmv CO, 50 ppmv HCl, and 24 ppbv $Hg^0$. The total flow of the simulated flue gas was 2 L/min. Elemental mercury vapor was supplied using a VICI Metronics Dynacalibrator permeation oven held at 100 °C and using $N_2$ as the carrier gas. The mercury concentration was higher than typical for a coal combustion flue gas to accommodate the sensitivity of the mercury analyzer and to ensure adequate loading on the adsorbent materials. Each sorbent (1.5−3 g) was exposed to the flowing flue gas simulant at 140 °C for 6−12 h resulting in mercury loading that ranged from 50 to 185 mg/kg based on an elemental mercury mass balance. The exposure temperature (140 °C) was chosen to approximate the duct temperature at the point of sorbent injection (just upstream of a particulate matter control device). Previous tests using this simulated flue gas mixture have shown that there is no oxidation of mercury in the absence of a sorbent or catalyst surface (i.e., no homogeneous oxidation via reaction with HCl or other flue gas component) in this experimental system at the exposure temperature (140 °C).

**XPS Analysis.** X-ray photoelectron spectroscopy (XPS) was performed using the Kratos Analytical Axis Ultra XPS at the Shared Materials Instrumentation Facility (SMIF), an interdisciplinary user facility at Duke University (Durham, NC). The materials were loaded into the sample chamber on double-sided copper tape (3M) and pumped down overnight to a vacuum of $10^{-8}$ Torr. The XPS spectrum was analyzed using CasaXPS software and all spectra were calibrated to the binding energy of C 1s photoelectrons at 285.2 eV. Full characterization of the speciation of surface-bound mercury is likely limited using this technique as it is possible that weakly bound mercury species are removed in the high vacuum environment. The XPS spectra are likely to be only from chemisorbed mercury species on the carbon surface.

**XAS Analysis.** XANES and EXAFS spectra were collected using the MR-CAT (Sector 10 ID) beamline at the Advanced Photon Source (APS) at Argonne National Laboratory (ANL, Argonne, IL) and beamline X18B at the National Synchrotron Light Source (NSLS) at Brookhaven National Laboratory (BNL, Upton, NY). The APS electron storage ring operated at 7 GeV with a topup fill status. The NSLS electron storage ring was operated at 2.528 GeV with beam currents in the 180−310 mA range. Both beamlines employed in the study utilized a Si(111) double-crystal monochromator. Experimental procedures were similar at both locations. XAS spectra were collected at the K absorption edge for Br (13 475 eV) and at the $L_{III}$ absorption edge (12 284 eV) for Hg. The K-edge XAS spectra for Cl and S were also of interest for these materials; however, these low energy absorption edges were below the energy ranges of the available beamlines that were used in this study. A series of reference mercury compounds (all are ACS reagent grade from Sigma-Aldrich except the $HgCl_2$ which was Puratrem grade from Strem Chemicals) were mounted as thin smears on Kapton (polyimide) tape for collection of transmission and fluorescence spectra using a Lytle detector at APS and a PIPS (passivated implanted planar silicon) detector at NSLS. At both locations a 13-element germanium array detector was used to collect fluorescence spectra from the activated carbon sorbent samples which were much more dilute in Hg content than the reference compounds. Multiple scans were used to improve the signal-to-noise ratio. The powdered activated carbon samples were loaded into thin Teflon sample holders between layers of Kapton tape.

## Results and Discussion

**Data Analysis.** Analysis of XAS data was performed following standard procedures using Athena and Artemis interfaces to the Iffefit software (*16*). The XAS spectrum was divided into two separate regions: the X-ray absorption near-edge structure (XANES) region and the extended X-ray absorption fine structure (EXAFS) region. The XANES technique is similar to other fine structure techniques except that the fine structure within a short energy range of the excitation threshold is measured. The XANES region can be viewed in two distinct parts: that just below and that just above the threshold $E_0$ ionization energy. The energies of the bound excited states in the preedge region are of primary interest for this work as interatomic transitions to Rydberg-like states are expected to be found in the threshold or low-energy part of the XANES region (*17*). Analysis of the XANES region was done by taking the first derivative of the spectrum [d(Abs)/d$E$] and plotting versus energy. Inflections in the preedge

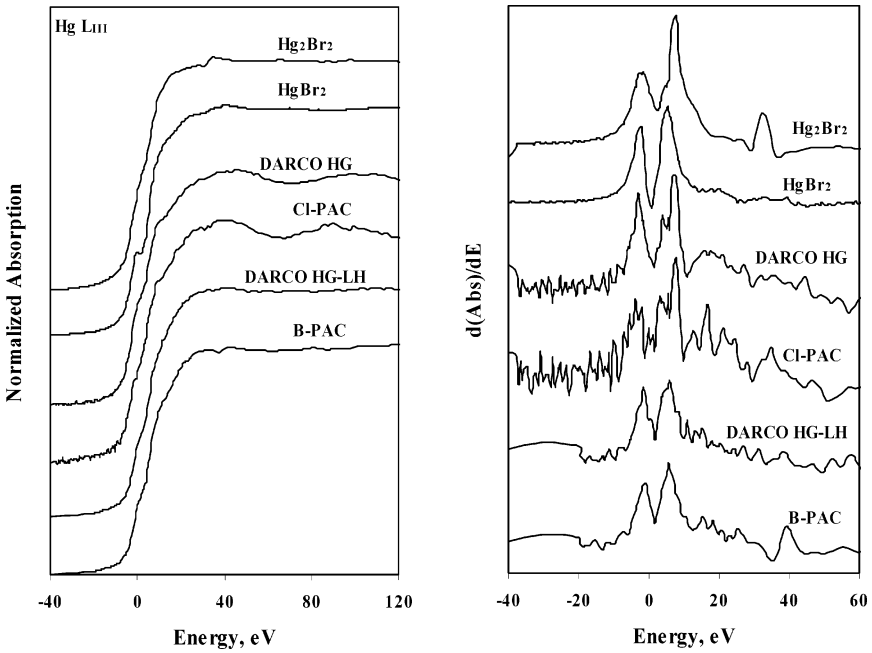


**FIGURE 1. Mercury $L_{III}$-edge XANES spectra (left) and first derivative of the spectra (right) for reference brominated mercury compounds and activated carbon sorbents ($E_0$ = 12,284 eV).**

XANES region are seen as two distinct peaks in the first derivative spectrum and the separation of the inflection points, termed the inflection point difference (IPD), can be determined (*11*, *12*). This IPD parameter can be used as an indicator of the local structure and bonding chemistry of Hg in the reference materials (and hence the local structure and bonding chemistry of Hg species on adsorbent materials). The separation of the Hg XANES inflection points likely depend on symmetry and coordination number, as well as the nature of the Hg−NN bond. However, as Huggins et al. (*12*) have emphasized, the IPD parameter is a single, average value that may reflect many bonding sites for mercury sorption; and as a result, may be less useful for complex samples, where binding may occur on a number of different sites.

The EXAFS region was analyzed by applying a Fourier transform to the EXAFS chi-function [$\chi$(k)] to obtain the radial structure function (RSF). This RSF can be regarded as a one-dimensional representation of the local structure around the absorbing atom and is known to correlate with the bond distance between the mercury atom and its nearest neighbor atoms (*12*).

**Hg XAS.** The XAS spectra were collected for the mercury−bromine salts ($HgBr_2$ and $Hg_2Br_2$) and mercury-containing activated carbon sorbents. The Hg $L_{III}$-edge XANES spectra for these materials are shown in Figure 1. Similar spectra were also collected for numerous other reference mercury compounds. These spectra were very similar to those which have been already been provided by Huggins et al. (*11*, *12*) and are, therefore, not shown here.

The most notable and distinguishing features of those reference compound spectra were the inflection points on the mercury preadsorption edge which were less prominent for the $Hg^{+1}$ species (e.g., $Hg_2Cl_2$ and $Hg_2SO_4$) and more pronounced for the $Hg^{2+}$ species. This is also evident for the $HgBr_2$ and $Hg_2Br_2$ spectra shown in Figure 1. However, none of the XANES spectra for the activated carbon samples display the obvious preedge features of the reference standards. The spectra for the brominated activated carbons (B-PAC and DARCO Hg-LH) appear smoother than those of the chlorinated (Cl-PAC) and the conventional (DARCO Hg) carbons which have more of an oscillating appearance in the area just above the threshold $E_0$ ionization energy. This postedge aspect is similar to that of the spectra for $HgCl_2$ and for the spectra of the other $Hg^{2+}$ reference compounds (HgO, $HgSO_4$, HgS).

**TABLE 1. XAFS Features for Hg Reference Compounds and Activated Carbon Sorbents**

| reference compound | first derivative XANES peak separation (eV) | RSF peak position (Å) |
|---|---|---|
| HgO (red) | 13.2 | 1.69 |
| $HgSO_4$ | 11.4 | 1.75 |
| $Hg(NO_3)_2$ (aq) | 10.7 | 1.75 |
| $Hg_2SO_4$ | 9.6 | 2.30 |
| $Hg_2Br_2$ | 8.8 | 2.42 |
| $Hg_2Cl_2$ | 8.1 | 2.00 |
| $HgCl_2$ | 8.0 | 1.85 |
| $HgBr_2$ | 7.7 | 2.11 |
| HgS (red) | 7.4 | 1.97 |
| $HgI_2$[a] | 6.5 | 2.61 |
| B-PAC | 6.8 | 2.10 |
| DARCO HG-LH | 7.5 | 1.98 |
| DARCO HG | 10.4 (7.1) | 1.93 |
| Cl-PAC | 11.4 (7.6) | 1.93 |

[a] These values are from references 11 and 12.

As described earlier, the inflections in the preedge XANES region are seen as two distinct peaks in the first derivative spectrum, also shown in Figure 1. The separation of these inflection points (the IPD) generally correlates with differences in the ionic nature of the Hg bonding. Table 1 gives the IPDs and RSFs for the reference mercury compounds. The largest values of the IPD are for HgO and those in which the Hg ion is surrounded by relatively small, oxygen-containing anions ($HgSO_4$, $H_2SO_4$, and $HgNO_3$). The mercury halides then fall in the midrange of IPD. Most interesting is the large difference in the IPD values of the $HgBr_2$ and the $Hg_2Br_2$ samples (7.7 and 8.8 eV respectively) as compared to the very similar values for $HgCl_2$ and $Hg_2Cl_2$ (8.0 and 8.1 eV respectively). Note that derivative XANES spectra for $Hg_2Br_2$ (Figure 1) is clearly different from that of the other standards in that it exhibits two unusually sharp peaks. $Hg_2Br_2$ was the only reference standard spectrum collected at BNL/NSLS

(the others were collected at ANL/APS). However, the same collection procedure was followed at both locations and should not be expected to affect the quality of the data. Huggins et al. have previously reported very similar values for both chloride salts and an IPD value of 6.5 eV for $HgI_2$ (*11*, *12*). The RSF values, not corrected for phase shift, generally trend as an inverse correlation to the IPD values (though not strictly). For the Hg halides the RSF values predictably trended with the size of the halide: $HgI_2 > HgBr_2 > HgCl_2$ and $Hg_2Br_2 > Hg_2Cl_2$. The HgX RSF values are larger than those of $HgX_2$ salts. Both of these trends are consistent with calculated and experimental values of bond distances (Hg−X) (*18*). Experimental Hg−X bond distances have been reported as $Hg_2Cl_2 = 2.42$ Å, $HgCl_2 = 2.25$ Å, $Hg_2Br_2 = 2.62$ Å, and $HgBr_2 = 2.41$ Å (*18*).

As with the XANES spectra, there is an obvious difference in the appearance of the derivative spectra for the brominated activated carbons as compared to the chlorinated and conventional materials (Figure 1). The derivative spectra for the Cl-PAC and the DARCO-HG carbon are more complex and contain unusually sharp peaks (this is likely a result of less Hg bound to the surface of these materials). In Table 1 the IPD values from the largest peaks for the Cl-PAC and the DARCO-HG derivative spectra are 11.4 and 10.4 eV, respectively, which are much higher than those of the brominated carbons (B-PAC at 6.8 eV and DARCO Hg-LH at 7.5 eV) and also much higher than the Hg-halide salts (also given in Table 1). Since there are lesser peaks just to the left of the largest peak for the Cl-PAC and the DARCO-HG samples, IPD values using those peaks were also calculated and are given in parentheses in Table 1. While the lower IPD values and the RSF peak position is more consistent with that of $HgCl_2$ (as one would expect) and HgS, the larger IPD values and the appearance of the XANES spectra for both the DARCO-HG and Cl-PAC sorbents suggests that some mercury may be bound to sulfate species that have been incorporated onto the carbon from $SO_2$ in the flue gas simulant. This is consistent with the findings of Huggins et al. (*11*) who found sulfate species along with HCl on the surface of lignite-based activated carbon sorbents that had been exposed to a synthetic flue gas. Since homogeneous oxidation has not been observed in this system, the mechanism of capture for these sorbents is likely to consist of surface-enhanced (heterogeneous) oxidation of the elemental mercury vapor via interaction with surface-bound chlorine species (most likely HCl) with subsequent binding by surface chloride and sulfate species. However, this may depend upon the specific conditions as Huggins et al. (*11*), using a lignite-based activated carbon, found that $SO_2$ (as $H_2SO_4$) and especially HCl enhance the sorption of elemental mercury, but found no evidence of the formation of surface mercury sulfates.

The mercury-containing brominated sorbents, however, seem to have IPD and RSF values—as well as a general aspect of their XANES spectra—that are consistent with those of the $HgBr_2$ reference standard (though also similar to those of the HgS reference).

**Br XANES.** The Br K-edge XANES spectra for the Hg−Br salts and brominated activated carbon sorbents are shown in Figure 2. The Br K-edge XANES spectra for the brominated activated carbon sorbents (including the DARCO Hg-LH which had not been exposed to mercury vapor) have a similar appearance with an immediate oscillation at the absorption edge ($E_0$). This is in contrast to the XANES spectra for the Hg−Br reference compounds which show noticeable but only slight oscillation at the absorption edge. This is not an unexpected result since only a very small portion of the brominated sites on the activated carbon are associated with bound mercury and the Br K-edge spectra is then dominated by those unassociated sites. Therefore, the Br K-edge XANES spectra are not useful in determining mechanisms or sites for mercury bound on these brominated activated carbon sorbents.

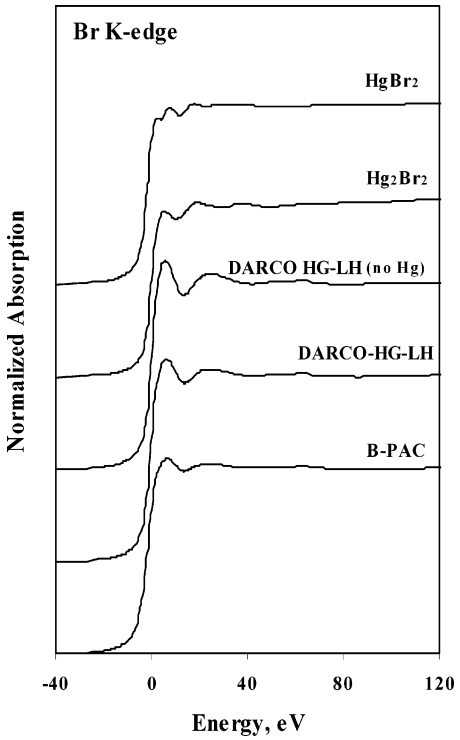


**FIGURE 2. Bromine K-edge XANES spectra for reference Hg−Br salts and brominated activated carbon sorbents ($E_0$ = 13,475 eV).**

**XPS Analysis.** The Hg 4f core level XPS spectra for Hg−Br reference salts and mercury-containing activated carbon sorbents are shown in Figure 3. A summary of the XPS Hg and Br binding energies for Hg−Br reference compounds and for mercury-containing activated carbon sorbents is given in Table 2. Literature values (*19*) for binding energies of mercury and Hg−Br compounds are also given for comparison in Table 2.

It is difficult to speciate mercury compounds using XPS analysis since the $4f_{7/2}$ binding energy for the most common reference materials range only from 99.9 to 101.4 eV (for $Hg^0$ and $HgCl_2$ respectively) and the ΔeV (the distance between the $4f_{5/2}$ and $4f_{7/2}$ peaks) is consistently $4.1 \pm 0.1$ eV. However, there is information that can be inferred from the spectra shown in Figure 3 and from the data presented in Table 2. It appears, consistent with the XAS results, that there is no elemental mercury adsorbed on the activated carbon samples since all of the $4f_{7/2}$ peaks are clearly shifted beyond the 99.9 eV reference point for $Hg^0$. This, along with the prior confirmation that there is no homogeneous mercury oxidation in the reactor system, indicates that there must be heterogeneous oxidation with subsequent (or concomitant) binding on the surface of the activated carbon. In the case of the conventional activated carbon (DARCO Hg), the oxidation likely involves HCl or $SO_2$ (as $H_2SO_4$) that is incorporated from the flue gas. The higher binding energies for the mercury on the activated carbons, as compared to those of the reference mercury halides and previously published values for elemental mercury, strongly suggest that the mercury is bound on the carbon at the chlorinated or brominated sites.

The Br 3d core level XPS spectra for Hg−Br reference salts and for mercury-containing DARCO Hg-LH activated carbon sorbent is also shown in Figure 3. As was the case with the Br XANES spectra, the Br XPS data are likely not useful for determining mechanisms or sites for mercury binding due to the low coverage of mercury on the brominated sites and,

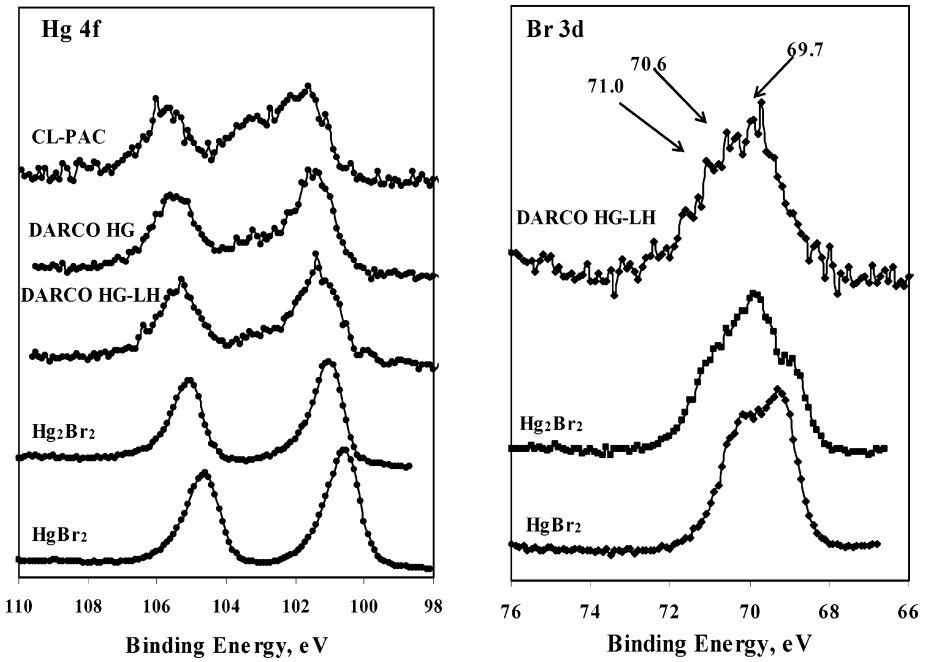


**FIGURE 3. Hg 4f (left) and Br 3d (right) core level XPS spectra for Hg−Br reference salts and activated carbon sorbents. (Note: No mercury-containing B-PAC sorbent was available at the time of XPS measurement)**

**TABLE 2. XPS Binding Energies for Hg−Br Reference Salts and for Mercury-containing Activated Carbon Sorbents**

| | binding energy, eV | | | | |
|---|---|---|---|---|---|
| | mercury (this study) | | | mercury (ref 19) | bromine[a] |
| sample | $4f_{5/2}$ | $4f_{7/2}$ | ΔeV | $4f_{7/2}$ | $3d_{5/2}$ |
| $Hg^0$ | | | | 99.9 | |
| $HgCl_2$ | | | | 101.4 | |
| $HgI_2$ | | | | 100.7 | |
| $HgBr_2$ | 104.6 | 100.5 | 4.1 | 101.0 | 69.3 |
| $Hg_2Br_2$ | 105.0 | 100.0 | 4.0 | 100.7 | 69.8 |
| DARCO-HG-LH | 105.3 | 101.4 | 3.9 | | 69.7 |
| DARCO-HG | 105.6 | 101.6 | 4.0 | | |
| Cl-PAC | 105.6 | 101.6 | 4.0 | | |

[a] Note: The Br 3d core level spectra (shown in Figure 3) have several small subpeaks which may represent different bonding environments within the bulk sample. In this table only the peak binding energy is given.

as such, the Br XPS spectra most likely reflect bromine at unassociated sites. The spectrum for the DARCO Hg-LH sample is, however, useful for understanding the binding of bromine to the carbon surface. This spectrum, shown in Figure 3, appears to have peaks in the Br 3d region at 69.7, 70.6, and 71.1 eV indicating that the bromine is bound to the surface at different sites. This has previously been noted in XPS studies involving brominated carbon materials (*20*−*22*). The binding energy peaks for the DARCO Hg-LH carbon were very similar to those measured for brominated single-walled carbon nanotubes (67.6 and 70.0 eV) (*21*) and for activated carbon (68.5 and 70.8 eV) (*22*)

Papirer and co-workers (*20*) found that different bromine bonds are detected depending on the bromination method and subsequent heat treatment. They used various bromination techniques and heat treatments in order to resolve the types of bromine bonds given by the Br XPS spectrum for brominated carbon black. The Br $3d_{5/2}$ peak at 70.0 ± 0.2 eV was attributed to bromine covalently bonded to sp2 and sp3 carbon atoms. Physisorbed HBr produced a $3d_{5/2}$ peak that varied between 67.8 ± 0.2 eV and 69.2 ± 0.2 eV. This weakly held component was eliminated after prolonged vacuum exposure at 100 °C and was no longer detectable after heating to 450 °C. The most strongly retained Br (resisted heating at 450 °C and was insensitive to aging) produced a peak at 67.4 ± 0.2 eV, which is significantly lower than the binding energies encountered with $Br^-$ compounds and was attributed to $C_n \rightarrow Br$ surface complexes. The $3d_{5/2}$ binding energies in the range of 76−78 eV were attributed to oxybrominated derivatives ($BrO_3^-$ and $BrO_4^-$). Based on this analysis and comparison to the Br $3d_{5/2}$ spectrum in Figure 3, it seems that the Br on the DARCO Hg-LH activated carbon can be attributed to bromine covalently bonded to sp2 and sp3 carbon atoms. It is also possible that there is physisorbed HBr present, though it would seem unlikely to withstand the vacuum pretreatment.

## Acknowledgments

Much of this work was performed at the U.S. EPA and supported, in part, by the appointment of Brian Attwood to the Postdoctoral Research Program at the National Risk Management Research Laboratory, administered by the Oak Ridge Institute for Science and Education (ORISE) through an Interagency Agreement BW89938167 between the U.S. Department of Energy (DOE) and the U.S. EPA. Mark Walters of Duke University's Shared Materials Instrumentation Facility (SMIF) performed the XPS measurements. MRCAT operations are supported by the Department of Energy and the MRCAT member institutions. Use of the Advanced Photon Source (APS) and National Synchrotron Light Source (NSLS) was supported by the U.S. DOE, Office of Science, Office of Basic Energy Sciences, under contract no. W-31-109-ENG-38 (APS/ANL) and contract no. DE-AC02-98CH10886 (NSLS/BNL). We acknowledge the through critique and helpful comments of the manuscript reviewers. Mention of trade names of commercial products and companies does not constitute endorsement or recommendation for use.

## Literature Cited

(1) For additional information regarding the health effects of mercury exposure and details of the Clean Air Mercury Rule (CAMR) see: www.epa.gov/mercury.

(2) Srivastava, S. K.; Hutson, N. D.; Martin, G. B.; Princiotta, F.; Staudt, J. Control of mercury emissions from coal-fired electric utility boilers. *Environ. Sci. Technol.* **2006**, *41*, 1385.

(3) Niksa, S.; Fujiwara, N. Predicting extents of mercury oxidation in coal-derived flue gases. *J. Air Waste Manage. Assoc.* **2005**, *55*, 930.

(4) Sanchez, F.; Keeney, R.; Kosson, D.; Delapp, R.; Thorneloe, S. Characterization of Mercury-Enriched Coal Combustion Residues from Electric Utilities Using Enhanced Sorbents for Mercury Control, US EPA Report EPA/600/R-06/008; U.S. Environmental Protection Agency: Washington, DC, 2006.

(5) Behra, P.; Bonnissel-Gissinger, P.; Alnot, M.; Revel, R.; Ehrhardt, J. J. XPS and XAS study of the sorption of Hg(II) onto pyrite. *Langmuir* **2001**, *17*, 3970.

(6) Kim, C. S.; Brown, G. E.; Rytuba, J. J.; Characterization and speciation of mercury-bearing mine wastes using X-ray absorption spectroscopy. *Sci. Total Environ.* **2000**, *261*, 157.

(7) Collins, C. R.; Sherman, D. M.; Ragnarsdottir, K. V. Surface complexation of $Hg^{2+}$ on goethite: Mechanism from EXAFS spectroscopy and density functional calculations. *J. Colloid Interface Sci.* **1999**, *219*, 345.

(8) Kim, C. S.; Rytuba, J. J.; Brown, G. E. (a) EXAFS study of mercury-(II) sorption to Fe- and Al-(hydr)oxides I. Effects of pH. *J. Colloid Interface Sci.* **2004**, *271*, 1. (b) EXAFS study of mercury(II) sorption to Fe- and Al-(hydr)oxides II. Effects of chloride and sulfate. *J. Colloid Interface Sci.* **2004**, *270*, 9.

(9) Brigatti, M. F.; Colonna, S.; Malferrari, D.; Medici, L.; Poppi, L. Mercury adsorption by montmorillonite and vermiculite: a combined XRD, TG-MS and EXAFS study. *Appl. Clay Sci.* **2005**, *28*, 1.

(10) Lennie, A. R.; Charnock, J. M.; Pattrick, R. A. D. Structure of mercury (II)-sulfur complexes by EXAFS spectroscopic measurements. *Chem. Geol.* **2003**, *199*, 199.

(11) Huggins, F. E.; Huffman, G. P.; Dunham, G. E.; Senior, C. L. XAFS examination of mercury sorption on three activated carbons. *Energy Fuels* **1999**, *13*, 114.

(12) Huggins, F. E.; Yap, N.; Huffman, G. P.; Senior, C. L. XAFS characterization of mercury captured from combustion gases on sorbents at low temperatures. *Fuel Proc. Tech.* **2003**, *82*, 167.

(13) Laumb, J. D.; Benson, S. A.; Olson, E. A. X-ray photoelectron spectroscopy analysis of mercury sorbent surface chemistry. *Fuel Process. Technol.* **2004**, *85*, 577.

(14) Olson, E. S.; Crocker, C. R.; Benson, S. A.; Pavlish, J. H.; Holmes, M. J. Surface compositions of carbon sorbents exposed to simulated low-rank coal flue gases. *J. Air Waste Manage. Assoc.* **2005**, *55*, 747.

(15) Ghorishi, S. B.; Keeney, R. M.; Serre, S. D.; Gullett, B. K.; Jozewich, W. S.; Development of a Cl-impregnated activated carbon for entrained-flow capture of elemental mercury. *Environ. Sci. Technol.* **2002**, *36*, 4454.

(16) Ravel, B.; Newville, M. ATHENA, ARTEMIS, HEPHAESTUS: Data analysis for X-ray adsorption spectroscopy using IFEFFIT. *J. Synchrotron Radiat.* **2005**, *12*, 537.

(17) Akesson, R.; Persson, I.; Sandstrom, M.; Wahlgren, U. Structure and bonding of solvated mercury(II) and thallium(III) dihalide and dicyanide complexes by XAFS spectroscopic measurements and theoretical calculations. *Inorg. Chem.* **1994**, *33*, 3715.

(18) Tossell, J. A.; Calculation of the energetics for oxidation of gas-phase elemental Hg by Br and BrO. *J. Phys. Chem. A* **2003**, *107*, 7804.

(19) Briggs, D.; Seah, M. P. *Practical Surface Analysis (Appendix 5)*; John Wiley & Sons, Inc., New York, 1996.

(20) Papirer, E.; Lacroix, R.; Donnett, J.-B.; Nanse, G.; Fioux, P. XPS study of the halogenation of carbon black—Part 1. bromination, *Carbon* **1994**, *32*, 1341.

(21) Duesberg, G. S.; Roth, S.; Downes, P.; Minett, A.; Graupner, R.; Lothar, L.; Nicoloso, N. Modification of single-walled carbon nanotubes by hydrothermal treatment, *Chem. Mater.* **2003**, *15*, 3314.

(22) Budarin, V. L.; Clark, J. H.; Tavener, S. J.; Wilson, K. Chemical reactions of double bonds in activated carbon: Microwave and bromination methods, *Chem. Commun.* **2004**, 2736.

*Received for review September 6, 2006. Revised manuscript received December 18, 2006. Accepted January 8, 2007.*

ES062121Q